Grinrey Conference Proceedings
Volume 01 (2026) 001201

ICMESR 2026, India, 04-05 May 2026
https://doi.org/10.55084/gcp/001201

# Design and Testing of a Modular Autonomous Delivery Robot for Healthcare and Industrial Service

Aaryaman Kochar[1,*], Girija Dahimiwal[1] and Vilas Kanthale[1]

[1]Department of Mechanical Engineering, MIT World Peace University, Pune, India

Email: aaryamankochar2005@gmail.com ([*]Corresponding Author)

Received : 15 Jun 2026; Accepted : 26 Jul 2026; Published : 08 Aug 2026

**Abstract.** The increased need for inexpensive intelligent robotic systems with autonomous capabilities in structured environments such as hospitals and warehouses has led to many innovations in the field of service robotics. This paper describes the design, development, and testing of a modular robot for autonomous delivery tasks featuring a four-wheeled differential drive chassis and ATmega328P microcontroller. The robot utilizes a combination of line-following using infrared sensors, object detection by ultrasonic sensors, smartphone Bluetooth control, and remote infrared controls on the same cost-effective platform. The robot has been successfully tested both in hardware and in Gazebo–ROS simulation, demonstrating the ability to track the defined path and detect and evade objects in a structured indoor environment. While the present version of the robot does not incorporate localization and SLAM capability, the modular chassis structure with three layers enables easy incorporation of LiDAR, IMU sensor, and wheel encoder to provide full autonomy in future versions of the robot.

**Keywords:** *Autonomous navigation; differential drive; line following; modular robotics; obstacle avoidance.*

## 1. INTRODUCTION

Autonomous systems are increasingly being used in logistics, health care, and manufacturing. There is therefore a need for an affordable autonomous robotic platform that can navigate within internal structures while having limited human interaction. Autonomous Delivery Robots (ADRs) are a rapidly expanding market sector of the Service Robotics Industry and have been recognized as a potential disruptor of last-mile logistics, intra-facility component transportation, and workplace automation. As reported by the International Federation of Robotics [1], the demand for service robotics continues to grow globally.

The autonomous mobile robot developed during this research project demonstrates many of the mathematical and structural design architectures inherent to industrial-grade ADRs, but at a significantly reduced price point. It features a structural aluminium frame, a four-wheel differential drive, an embedded hardware sensing array, and a programmable microcontroller board, all of which mirror its commercial counterparts. Autonomous navigation is based on a combination of theories that revolve around kinematics, localization, mapping, and motion planning [2, 3]. These principles ensure that mobile robots achieve optimal stability and accurate paths while moving around autonomously.

Hardware-wise, the ATmega328P has been adopted widely in small-scale robotics [4] to provide cheap and deterministic real-time processing capabilities via dual H-Bridge motor driver ICs, such as the L293D [5], allowing bidirectional operation of differential DC motors. Recent academic trends move reactive robotic prototypes toward highly scalable and intelligent robots fit for real-world applications. This is usually achieved using multi-sensor fusion frameworks, advanced path planning algorithms such as A* and


ISBN: 978-81-996627-3-5

Dijkstra's algorithm [6, 7], and middleware layers such as the Robot Operating System (ROS) [8]. By detecting obstacles and collecting data from multiple sensors simultaneously, the system in this paper provides a hardware/software platform that avoids unnecessary functionality while remaining scalable across multiple future platforms.

Modern day research supports this observation. For example, a review conducted in 2024 assessed the prospective use of autonomous last mile delivery robots and revealed the existence of serious barriers preventing their introduction on a large scale [9]. In particular, healthcare sector can greatly benefit from mobile robots as demonstrated by a benchmarking study published in 2024 which confirmed limited number of conducted trials and the absence of standardized testing protocols in this area [10]. Another paper released in 2024 emphasized the growing number of small-drive vehicles used in transportation logistics in warehouse structures [11]. Additionally, in 2024 the construction of a low-cost vehicle based on microprocessors and microcontrollers proved that it is possible to develop and apply economical devices for autonomous solving of common tasks in practice [12]. There was also a study published in 2024 examining potential uses of delivery vehicles, bicycles and vans in fourteen cities in Europe that revealed the possibility of applying small-size autonomous vehicles' techniques for transportation in the 'last mile' (short-distance journey) [13]. Finally, a paper published in 2025 confirmed the importance of low-cost designs in health care robotics [14]. The present paper aims to fill this gap by describing a low-cost delivery robot successfully tested in both field and simulation.

## 2. METHODS

### 2.1 Design Considerations and Hardware Architecture

The self-driving delivery robot is built as a small and modular mobile base for effective operation in flat, structured indoor spaces. The locomotive frame is a four-wheel differential drive mechanism, which can achieve forward, backward, left-turn, right-turn, and in-situ rotation motion without a mechanical steering system. The major design points are:

- Balance: Bulky battery packs are located at the center of the vehicle to maintain a low center of gravity and good balance during sudden direction changes.
- Lightweight Frame: Tailor-made aluminium plates provide mechanical strength and structural integrity while reducing curb weight.
- Modularity: A three-layer chassis – base plate, middle plate, top plate – facilitates simple assembly, separated maintenance, and future hardware additions.
- Economical: An Arduino Nano board with simple discrete sensors substantially reduces overall system cost.
- User-Friendly Operation: An IR remote and a Bluetooth module together provide dual-control capability to the user.

### 2.2 Mechanical and Electrical Assembly

The mechanical assembly follows a detailed, phased modular process. Four DC geared motors are first fastened to the main aluminium base plate with four M3×30 mm bolts and nuts. High-traction 65 mm rubber-tyred wheels are then connected directly to the motor shafts, maintaining coaxiality. The IR line-tracking sensors are mounted on a dedicated front IR mount with M3×10 mm bolts, positioned at the front-bottom of the chassis facing the ground. A dedicated vertical bracket holds the HC-SR04 ultrasonic sensor at the very front of the robot. The battery box is fixed at the geometric center of the base plate for balanced weight distribution. Hexagonal metallic spacers connect the base plate to the upper structural layers: the middle plate is fastened onto these spacers and the custom controller PCB is mounted on top of it, and the upper plate is fixed last to complete the three-layer structure.

To clarify the overall signal and power flow between these components, Figure 1 presents a block diagram of the complete system architecture, showing how the sensing, control, actuation, communication, and power subsystems are interconnected around the ATmega328P microcontroller.

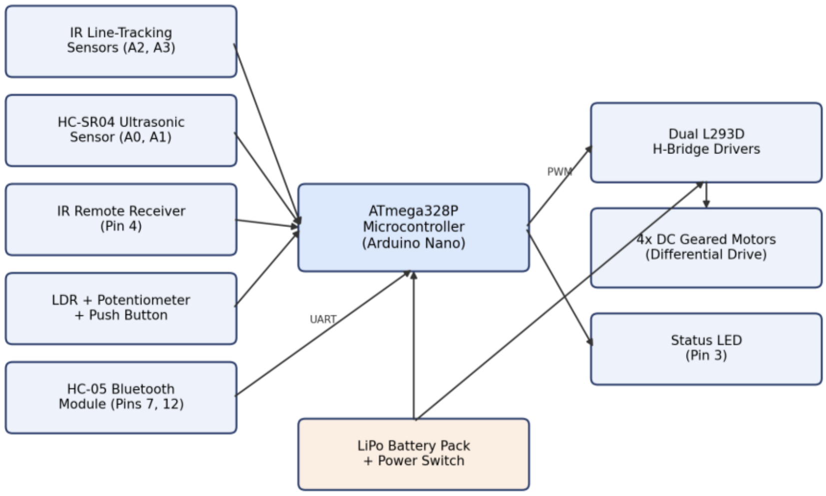


**Fig. 1** System architecture and signal-flow block diagram of the modular autonomous delivery robot.

Table 1 summarizes every sensor and actuator connection to the ATmega328P. Locomotion is handled through two PWM-capable pins driving the left and right motor pairs via the L293D drivers, while the two IR line sensors and the ultrasonic trigger/echo pair occupy four analog input pins. The remaining pins are reserved for the Bluetooth UART link, status LED, mode button, calibration potentiometer, ambient-light sensor, and an unused I2C bus kept free for future sensor expansion (see Section 4.4).

**Table 1.** Controller Pin Configuration and Wiring Topology

| Sr. | Subsystem | Component | Pin | Function |
|---|---|---|---|---|
| 1 | Locomotion | Motors 1&2 (Left) | PWM ~5, D6, D8 | Left speed/direction |
| 2 | Locomotion | Motors 3&4 (Right) | PWM ~10, D11, D13 | Right speed/direction |
| 3 | Line Tracking | Left IR sensor | A2 | Left surface contrast |
| 4 | Line Tracking | Right IR sensor | A3 | Right surface contrast |
| 5 | Obstacle Avoidance | Ultrasonic trigger | A0 | 40 kHz burst emit |
| 6 | Obstacle Avoidance | Ultrasonic echo | A1 | Reflected echo receive |
| 7 | Manual Control | IR remote receiver | D4 | 38 kHz NEC decode |
| 8 | Telemetry | HC-05 Bluetooth | Rx D7 / Tx D12 | Smartphone UART |
| 9 | Feedback | Diagnostic LED | PWM ~3 | Status blinking |
| 10 | User Interface | Mode push-button | D2 | Manual mode select |
| 11 | Tuning | Potentiometer | A7 | Hardware calibration |
| 12 | Environment | LDR | A6 | Ambient light sampling |
| 13 | Expansion | I2C bus | A4 (SDA), A5 (SCL) | Future IMU/OLED |

Electrical wiring must be completed establishing good point to point wiring paths as per the pinout of the system. Each of the four DC motors is directly connected to the outputs of two integrated circuits of the type L293D (Dual H-Bridge motor driver), mounted on the circuit board, which provide all of the end-to-end bi-directional voltage control. Centralized system power routing and full electrical isolation are achieved via the provision of a high energy density rechargeable lithium polymer (LiPo) cell pack fed directly to the main dc power jack of the board through a mechanical toggle switch of the on board.

### 2.3 Kinematic Modeling and Locomotion

The robot's motion is governed by standard two-dimensional differential-drive kinematics [1, 2]. By varying the individual rotational velocities of the left and right wheel pairs, the system executes straight-line trajectories, smooth curves, and zero-radius in-place turns. The forward linear velocity v of the robot's center of mass and its angular velocity ω about the vertical axis are derived from the individual velocities of the right wheel pair ($v_r$) and left wheel pair ($v_l$) via the following equations:

$$v = \frac{v_r + v_l}{2} \tag{1}$$

Equation (1) states that the robot's forward speed is simply the average of the two wheel-pair speeds, so if both pairs turn at the same rate the robot moves in a straight line. Equation (2) states that any difference between the right- and left-wheel speeds, divided by the wheel track L, produces a rotation: the larger the speed difference, the sharper the turn, and a reversed pair ($v_r = -v_l$) produces an in-place, zero-radius spin.

$$\omega = \frac{v_r - v_l}{L} \tag{2}$$

where L is the lateral distance between the left and right wheel contact points (L = 145 mm). Motor speed control is achieved by modulating the effective voltage applied via the L293D drivers using 8-bit Pulse Width Modulation (PWM) values bounded strictly between 0 (stalled) and 255 (maximum continuous torque).

### 2.4 Software Architecture and Control Algorithms

The embedded firmware is written within the Arduino C/C++ environment, utilizing an event-driven finite state machine structure that continuously polls sensor interfaces and executes reactive control loops.

**Table 2.** Closed-Loop Line Following Decision Logic

| Left IR (A2) | Right IR (A3) | Robot Action | Motor Vectors |
|---|---|---|---|
| White (high refl.) | White (high refl.) | Move straight forward | Both pairs forward |
| Black line (low refl.) | White (high refl.) | Sharp left turn | Left reverse, right forward |
| White (high refl.) | Black line (low refl.) | Sharp right turn | Left forward, right reverse |
| Black line (low refl.) | Black line (low refl.) | Full stop | Both pairs brake |

Table 2 lists the four possible combinations of the two IR line sensors and the resulting motor response. Because the sensors are mounted only 20 mm apart, the robot re-evaluates this table roughly every 5 ms, so it corrects small deviations from the line before they grow large enough to cause a full stop-and-recover event. In the autonomous Obstacle Avoidance Mode, the ultrasonic sensor continuously gauges the forward clearance distance [6] using a high-accuracy time-of-flight equation:

$$\text{Distance} = \frac{\text{Echo Time} \times \text{Speed of Sound}}{2} \tag{3}$$

The speed of sound was assumed to be about 343 m/s in the dry air at room temperature.
Equation (3) converts the round-trip time of the reflected ultrasonic pulse into a physical distance: the speed of sound (assumed 343 m/s in dry air at room temperature) is multiplied by the measured echo time and halved, since the pulse travels to the obstacle and back.

The Conditional Decision-Making Architecture uses this deterministic path to follow these routines:
(1) **Clear Path** — if distance > 20 cm, the robot continues forward at its normal speed
(2) **Obstacle** — if distance ≤ 20 cm, both motor pairs stop immediately
(3) **Evasion** — the robot performs an in-place turn for a fixed duration to change heading
(4) **Re-verification** — the sensor re-samples distance in the new heading, resuming forward motion once clear or continuing to turn otherwise.

## 3. RESULTS

### 3.1 Simulation Metrics and Outcomes

The ROS–Gazebo simulation environment was used to test the differential-drive kinematics and the closed-loop reactive control algorithms. The simulated vehicle followed a variety of paths in virtual worlds with relatively small tracking errors when commanded via /cmd_vel velocity inputs. All simulated physical barriers that would cause collisions were correctly detected, and the obstacle-avoidance algorithm reliably stopped the vehicle and generated a new heading before contact with a wall or barrier.

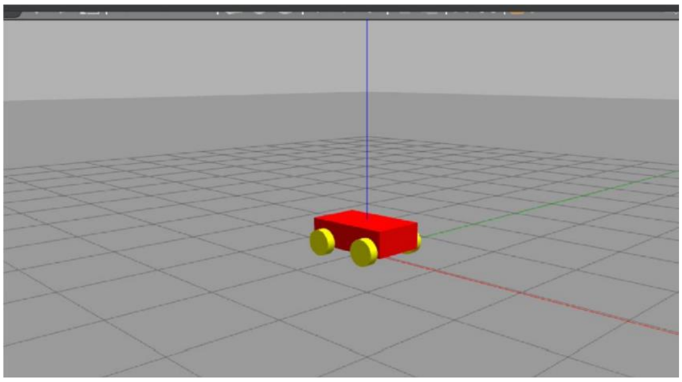

**Fig. 2** Gazebo simulation environment of the proposed modular autonomous delivery robot.

### 3.2 Hardware Performance and Functional Verification

After verifying the simulations, physical testing was performed on a prototype to evaluate real-world operational effectiveness across all four integrated operating modes.

**Table 3.** Empirical Functional Performance Matrix

| Function | Expected Outcome | Observed Result | Performance Metric |
|---|---|---|---|
| Line Following | Seamless adherence to black tape path | Successful tracking, zero deviations | Max deviation: ±12 mm |
| Obstacle Avoidance | Full stop & evasion before collision | Reliable stop and turn-away | Evasion within 20 cm window |
| IR Remote Control | Manual wireless direction/speed | Highly responsive directional control | Line-of-sight range up to 8.5 m |
| Bluetooth Control | Smartphone app command execution | Stable real-time UART link | Continuous range up to 10.2 m |
| Motor Control | Smooth, stepless speed variation | Successful PWM voltage modulation | 255 discrete linear steps |

Sensor validation trials confirmed that under ambient lighting conditions, the reflection threshold delta between the dark tracking lines and light floor tiles remained sufficiently high to prevent any tracking faults. The ultrasonic sensor exhibited a high degree of measurement accuracy within a functional range of 2cm to 400cm, with an empirical distance measurement resolution of approximately 3mm.

# 4. DISCUSSION

## 4.1 Performance Analysis and Synthesis

The physical and simulated data show that the prototype effectively combines multimodal sensing, real-time embedded processing, and dual-axis motion for indoor navigation. The low-complexity reactive algorithm executes at high speed on the ATmega328P, mapping sensor data directly to motor output without the computational overhead of a high-level operating system.

Real-world testing did identify differences between the idealized Gazebo simulation and actual performance. Variations in surface friction, motor manufacturing tolerances, wheel-hub misalignment, and minor electrical sensor noise caused slight heading deviations during long straight-line runs, which the line-following correction loop continually compensated for.

The results obtained represent a remarkable achievement in comparison with other cost-effective and microcontroller-based platforms described in the recent literature. A mobile robot created in 2024 for indoor surveillance and equipped with an Arduino-like controller around which a companion computer was installed demonstrated reliable obstacle avoidance and search capabilities, although it requires significantly greater computational and sensing infrastructure (an NVIDIA Jetson Nano) than the proposed solution [12]. According to the 2024 literature about autonomous delivery robots, the majority of the existing commercial ADRs use LiDAR-based SLAM systems approximately ten times more expensive than the friction-based systems while being in many cases accessible for learning and experimentation [9]. The robot described is characterized by lower costs of construction materials, a completely open control scheme for reactive navigation, thus making the device more suitable for classroom and research use, though not yet for the unstructured and dynamic environment of hospital corridors [10].

## 4.2 Discussion of System Characteristics and Future Enhancements

- Operational Versatility: Four functional modes provide multipurpose capability without physical reconfiguration. Redundant Communication: Two independent communication channels (Bluetooth UART and infrared NEC) provide a reliable backup if one method fails.
- Perception Blind Spots: The fixed, forward-facing ultrasonic sensor cannot sweep or rotate, so the robot is blind to objects behind or beside it, limiting its ability to plan around larger obstacles.
- Lack of Odometric Feedback: Without a wheel encoder or IMU, the robot cannot determine its absolute pose (x, y, θ) or detect wheel slippage.
- Physical Limits: The exposed aluminium frame restricts operation to clean, dry, flat, indoor floors, and is unsuitable for humid or dusty environments.
- Computational Limits: The ATmega328P (16 MHz, 32 KB flash, 2 KB SRAM) cannot store map data or process image data, and cannot run multiple tasks concurrently without an RTOS.
- Communication Gaps: Neither the Bluetooth module nor the IR receiver supports internet access or multi-node networking, so cloud connectivity or multi-robot coordination is not currently possible.

If the above described educational prototype is going to become an autonomous robotic delivery vehicle for commercial applications, then the following options should be considered for future development paths/enhancements: Advancements in the sensor technology explain that LiDAR sensor is nothing but a rapid rotating measuring instrument to measure the distances to all the walls and any items as well. With the help of LiDAR, it becomes possible for the robot to view the environment and eliminate visibility issues that have been discussed earlier. Conventionally, a small piece called IMU (inertial measuring unit) is there to detect tilt and speed of motion of the robot the same way as one obtains information about the current orientation of a smartphone; Its addition would be beneficial since combining different data collected via

LiDAR and IMU with the help of Extended Kalman Filter (EKF) would lead to an ability of the robot to measure its location and orientation continuously while moving, thus enabling it to direct itself properly.

- Future Nav Stack: Upgrade to a single-board computer (Raspberry Pi or NVIDIA Jetson) to run a full ROS navigation stack with AMCL localization and A* path planning.
- Future Sensor Fusion: Mount a 360° LiDAR and a 9-axis IMU, fused via EKF, to eliminate the single-sensor blind spots identified above.
- Future Closed-Loop Actuation: Install optical wheel encoders on all four motor shafts to enable precision closed-loop PID velocity control and accurate odometry.

## 5. CONCLUSION

This paper has presented a low-cost modular autonomous delivery robot designed for structured indoor environments (i.e., hospitals, warehouses), detailing the hardware assembly and testing procedures. The major novelty of this work did not rely on the use of any particular sensor or algorithm but on the combination of four control modes that operate separately: autonomous line following, obstacle avoidance, Bluetooth smartphone control, and IR remote control; all of which were implemented in one platform based on ATmega328P. Both simulation studies, and real-world experiments confirmed the successful operation of the navigation and autonomous obstacle detections, as well as practical two-mode control system. The three-layer modular chassis has been developed in such a way that the various equipment like LiDaR, IMU, and wheel encoders can be attached to it, which addresses localization and SLAM problems discussed previously in this paper.

## NOMENCLATURE AND ABBREVIATIONS

| | | | | | |
|---|---|---|---|---|---|
| ADR | : | Autonomous Delivery Robot | PWM | : | Pulse Width Modulation |
| AMCL | : | Adaptive Monte Carlo Localization | ROS | : | Robot Operating System |
| DC | : | Direct Current | RTOS | : | Real-Time Operating System |
| EKF | : | Extended Kalman Filter | SRAM | : | Static Random-Access Memory |
| I2C | : | Inter-Integrated Circuit | UART | : | Universal Asynchronous Receiver-Transmitter |
| IMU | : | Inertial Measurement Unit | URDF | : | Unified Robot Description Format |
| IR | : | Infrared | v | : | Forward linear velocity of robot center of mass |
| L | : | Lateral wheel-track distance (145 mm) | v_l | : | Linear velocity of the left wheel pair |
| LDR | : | Light Dependent Resistor | v_r | : | Linear velocity of the right wheel pair |
| LiPo | : | Lithium Polymer | ω | : | Angular velocity about the vertical axis |
| PCB | : | Printed Circuit Board | | | |

## REFERENCES


[1] International Federation of Robotics, *World Robotics 2025 – Service Robots*. Frankfurt, Germany: IFR, 2025. [Publisher].

[2] R. Siegwart, I. R. Nourbakhsh, and D. Scaramuzza, *Introduction to Autonomous Mobile Robots*, 2nd ed. Cambridge, MA, USA: MIT Press, 2011. [CrossRef] [Publisher]

[3] S. Thrun, W. Burgard, and D. Fox, *Probabilistic Robotics*. Cambridge, MA, USA: MIT Press, 2005. [CrossRef] [Publisher]

[4] Microchip Technology Inc., "ATmega328P Complete Datasheet," DS40002061, 2020. [CrossRef] [Publisher]

[5] Texas Instruments, "L293D Quadruple Half-H Drivers Datasheet," SLRS008C, Nov. 1986, Revised Jan. 2016. [Publisher].

[6] P. E. Hart, N. J. Nilsson, and B. Raphael, "A Formal Basis for the Heuristic Determination of Minimum Cost Paths," *IEEE Trans. Syst. Sci. Cybern.*, vol. 4, no. 2, pp. 100–107, Jul. 1968. [CrossRef] [Publisher]

[7] E. W. Dijkstra, "A note on two problems in connexion with graphs," *Numer. Math.*, vol. 1, no. 1, pp. 269–271, Dec. 1959. [CrossRef] [Publisher]

[8] P. Corke, *Robotics, Vision and Control: Fundamental Algorithms in MATLAB*, 2nd ed. Cham, Switzerland: Springer, 2017. [CrossRef] [Publisher]

[9] E. Alverhed, V. Hulten, and M. Browne, "Autonomous last-mile delivery robots: A literature review," *Eur. Transp. Res. Rev.*, vol. 16, no. 1, Art. no. 4, Jan. 2024. [CrossRef] [Publisher]

[10] C. Rondoni et al., "Navigation benchmarking for autonomous mobile robots in hospital environment," *Sci. Rep.*, vol. 14, no. 1, Art. no. 18334, Aug. 2024. [CrossRef] [Publisher]

[11] R. Keith and H. M. La, "Review of Autonomous Mobile Robots for the Warehouse Environment," *arXiv*, Art. no. 2406.08333, Jun. 2024. [CrossRef] [Publisher]

[12] S. U. Ahamad, M. Ataei, V. Devabhaktuni, and V. Dhiman, "Omobot: A Low-Cost Mobile Robot for Autonomous Search and Fall Detection," in *Proc. IEEE Int. Conf. Adv. Intell. Mechatron. (AIM)*, Jul. 2024, pp. 453–460. [CrossRef] [Publisher]

[13] A. Garus et al., "Unravelling the last-mile conundrum: A comparative study of autonomous delivery robots, delivery bicycles, and light commercial vehicles in 14 varied European landscapes," *Sustain. Cities Soc.*, vol. 108, Art. no. 105490, Sep. 2024. [CrossRef] [Publisher]

[14] H. Shin et al., "A Comprehensive Review of Autonomous Mobile Robots in Healthcare: Implications for Patient-Transporting Human-Following Robots," *Robotics*, vol. 14, no. 12, Art. no. 179, Dec. 2025. [CrossRef] [Publisher]